Article

Toward [F]-Labeled Aryltrifluoroborate Radiotracers: In Vivo Positron Emission Tomography Imaging of Stable Aryltrifluoroborate Clearance in Mice

Richard Ting, Curtis Harwig, Ulrich auf dem Keller, Siobhan McCormick, Pamela Austin, Christopher M. Overall, Michael J. Adam, Thomas J. Ruth, and David M. Perrin

J. Am. Chem. Soc., **2008**, 130 (36), 12045-12055 • DOI: 10.1021/ja802734t • Publication Date (Web): 14 August 2008

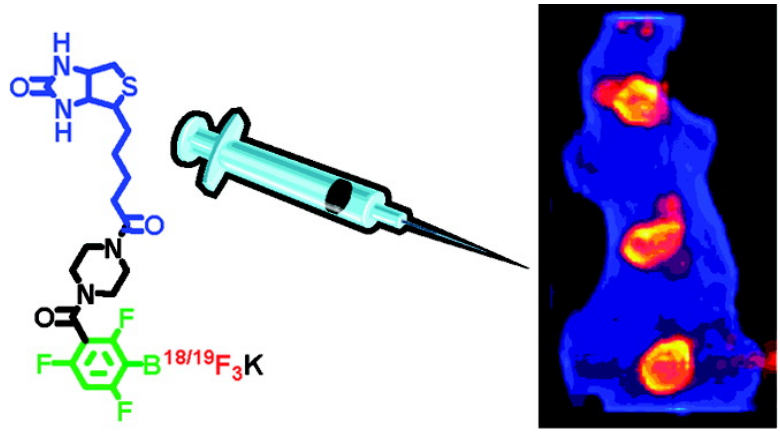

More About This Article

Additional resources and features associated with this article are available within the HTML version:

- Supporting Information
- Access to high resolution figures
- Links to articles and content related to this article
- Copyright permission to reproduce figures and/or text from this article

View the Full Text HTML

J|A|C|S
ARTICLES

Published on Web 08/14/2008

Toward [^{18}F]-Labeled Aryltrifluoroborate Radiotracers: In Vivo Positron Emission Tomography Imaging of Stable Aryltrifluoroborate Clearance in Mice

Richard Ting,[†] Curtis Harwig,[†] Ulrich auf dem Keller,[||] Siobhan McCormick,[§] Pamela Austin,[⊥] Christopher M. Overall,[||] Michael J. Adam,[†,‡] Thomas J. Ruth,[†,§] and David M. Perrin*[,†]

Chemistry Department, University of British Columbia, 2036 Main Mall, Vancouver, B.C. V6T-1Z1, Canada, PET Chemistry Group, TRIUMF, 4004 Wesbrook Mall, Vancouver, B.C. V6T-2A3, Canada, Department of Medicine, University of British Columbia, Vancouver, B.C. V6T-2B5, Canada, Centre for Blood Research, Life Sciences Centre, 2350 Health Sciences Mall, University of British Columbia, Vancouver, B.C. V6T-1Z3, Canada, and Department of Cellular and Physiological Sciences, Life Sciences Institute, University of British Columbia, 2350 Health Sciences Mall, Vancouver, B.C. V6T-1Z3, Canada

Received April 14, 2008; E-mail: dperrin@chem.ubc.ca

Abstract: The use of a boronic ester as a captor of aqueous [^{18}F]-fluoride has been previously suggested as a means of labeling biomolecules in one step for positron emission tomography (PET) imaging. For this approach to be seriously considered, the [^{18}F]-labeled trifluoroborate should be humorally stable such that it neither leaches free [^{18}F]-fluoride to the bone nor accumulates therein. Herein, we have synthesized a biotinylated boronic ester that is converted to the corresponding trifluoroborate salt in the presence of aqueous [^{18}F]-fluoride. In keeping with its in vitro aqueous kinetic stability at pH 7.5, the trifluoroborate appears to clear in vivo quite rapidly to the bladder as the stable trifluoroborate salt with no detectable leaching of free [^{18}F]-fluoride to the bone. When this labeled biotin is preincubated with avidin, the pharmacokinetic clearance of the resulting complex is visibly altered. This work validates initial claims that boronic esters are potentially useful as readily labeled precursors to [^{18}F]-PET reagents.

Introduction

Recently there has been considerable interest in imaging disease states such as cancer and inflammation, particularly with respect to specific cellular pathologies.[1−8] To do this, one needs to recognize a pathologically distinct cellular target (e.g., receptor, cell surface protein) with a ligand that manifests high specificity *and* high affinity in vivo. Such recognition properties are usually incumbent of moderately large molecules such as biotin,[9] folate,[10] octreotide,[11] and RGD,[12,13] macromolecules such as insulin,[14] EGF,[15] antibodies,[16] aptamers,[6] oligonucleotides,[17] and avidin-antibody fusion proteins, as well as avidin-mediated sandwiches that conjoin different biotinylated conjugates.[18]

To comprehend the in vivo fate of these ligands and to exploit their binding properties in vivo for the noninvasive visualization of disease states, one also needs a suitable photon emitting

[†] Chemistry Department, University of British Columbia.
[||] Centre for Blood Research, Life Sciences Institute 4401, University of British Columbia.
[§] Department of Medicine, University of British Columbia.
[⊥] Department of Cellular and Physiological Sciences, Life Sciences Institute, University of British Columbia.
[‡] TRIUMF.

(1) Torigian, D. A.; Huang, S. S.; Houseni, M.; Alavi, A. *CA-A Cancer J. Clin* **2007**, *57*, 206.
(2) Hoffman, J. M.; Gambhir, S. S. *Radiology* **2007**, *244*, 39.
(3) Mather, S. J. *Mol. Biosyst.* **2007**, *3*, 30.
(4) Mankoff, D. A.; Eary, J. F.; Link, J. M.; Muzi, M.; Rajendran, J. G.; Spence, A. M.; Krohn, K. A. *Clin. Cancer. Res.* **2007**, *13*, 3460.
(5) Adam, M. J.; Wilbur, D. S. *Chem. Soc. Rev.* **2005**, *34*, 153.
(6) Britz-Cunningham, S. H.; Adelstein, S. J. *J. Nucl. Med.* **2003**, *44*, 1945.
(7) Jaffer, F. A.; Weissleder, R. *J. Am. Med. Assoc.* **2005**, *293*, 855.
(8) Shoup, T. M.; Fischman, A. J.; Jaywook, S.; Babich, J. W.; Strauss, H. W.; Elmaleh, D. R. *J. Nucl. Med.* **1994**, *35*, 1685.
(9) Tannous, B. A.; Grimm, J.; Perry, K. F.; Chen, J. W.; Weissleder, R.; Breakefield, X. O. *Nat. Methods.* **2006**, *3*, 391.
(10) Dube, D.; Francis, M.; Leroux, J.-C.; Winnik, F. M. *Bioconjugate Chem.* **2002**, *13*, 685.
(11) Gabriel, M.; Decristoforo, C.; Kendler, D.; Dobrozemsky, G.; Heute, D.; Uprimny, C.; Kovacs, P.; Von Guggenberg, E.; Bale, R.; Virgolini, I. J. *J. Nucl. Med.* **2007**, *48*, 508.
(12) Chen, X.; Park, R.; Tohme, M.; Shahinian, A. H.; Bading, J. R.; Conti, P. S. *Bioconjugate Chem.* **2004**, *15*, 41.
(13) Haubner, R.; Kuhnast, B.; Mang, C.; Weber, W. A.; Kessler, H.; Wester, H. J.; Schwaiger, M. *Bioconjugate Chem.* **2004**, *15*, 61.
(14) Shai, Y.; Kirk, K. L.; Channing, M. A.; Dunn, B. B.; Lesniak, M. A.; Eastman, R. C.; Finn, R. D.; Roth, J.; Jacobson, K. A. *Biochemistry* **1989**, *28*, 4801.
(15) Fredriksson, A.; Johnstrom, P.; Thorell, J. O.; von Heijne, G.; Hassan, M.; Eksborg, S.; Kogner, P.; Borgstrom, P.; Ingvar, M.; Stone-Elander, S. *Life Sci.* **1999**, *65*, 165.
(16) Wu, A. M.; Yazaki, P. J.; Tsai, S. W.; Nguyen, K.; Anderson, A. L.; McCarthy, D. W.; Welch, M. J.; Shively, J. E.; Williams, L. E.; Raubitschek, A. A.; Wong, J. Y. C.; Toyokuni, T.; Phelps, M. E.; Gambhir, S. S. *Proc. Natl. Acad. Sci. U.S.A.* **2000**, *97*, 8495.
(17) Kuhnast, B.; de Bruin, B.; Hinnen, F.; Tavitian, B.; Dolle, F. *Bioconjugate Chem.* **2004**, *15*, 617.
(18) Cauchon, N.; Langlois, R.; Rousseau, J. A.; Tessier, G.; Cadorette, J.; Lecomte, R.; Hunting, D. J.; Pavan, R. A.; Zeisler, S. K.; van Lier, J. E. *Eur. J. Nucl. Med. Mol. Imaging* **2007**, *34*, 247.

functionality that is appended to the ligand via a robust bioconjugation strategy. Of the existing imaging modalities, positron emission tomography (PET) provides some of the highest resolution images within deep tissue due to two 180°-correlated 511 keV photons that are released upon annihilation of each positron (β^+). If PET is the imaging modality of choice, then from a nuclear perspective [^{18}F]-fluoride is the isotope of choice on account of its numerous desirable properties including a moderate half-life (110 min), low β^+-trajectory (<2 mm), a clean nuclear decay process (~97% β^+-emission), ready production from a stable heavy atom precursor, that is, ^{18}O-labeled gas and/or water, and facile isolation in relatively high isotopic purity.

From a radiosynthetic perspective however, the chemical incorporation of fluorine is problematic, particularly in regards to the direct labeling of large, water soluble, polyfunctional, and often temperature sensitive macromolecules.[19] Consequently, numerous indirect labeling strategies have appeared whereby an atom of [^{18}F]-fluorine, usually isolated as the anion, is first introduced onto a small organic precursor, which must suffer at least one, if not several more synthetic transformations terminating in bioconjugation. Most of these approaches involve the relatively restricted labeling strategies predicated on C−F bond formation, examples of which include nucleophilic displacement by fluoride on alkyltosylates, aryltrimethylammonium ions, and nitroaromatics.[17,20−24] Over the past 2 decades, much effort has been directed to generating electrophilic variants of the above and in optimizing the chemoselectivity in bioconjugation.[23,24]

Although no-carrier added syntheses have been successful with regards to the preparation of small organofluoride precursors, the subsequent bioconjugation to a large molecule is often not high yielding despite the fact that a vast excess of biomolecule is often added to drive the conjugation reaction forward. Moreover, because the separation of the unconjugated biomolecule from the desired conjugate can be difficult, there can be a significant reduction in the specific activity of the final product, that is, the Ci/μmol biomolecule. Despite significant advances in synthetic/bioconjugation methodologies,[23] the manipulation of dry anionic [^{18}F]-fluoride in the first synthetic step, elevated temperatures sometimes required during a subsequent bioconjugation step,[17] and the potential for both side reactions and overconjugation[14] all conspire to limit the practical application of [^{18}F]-labeled bioconjugates. Furthermore, the 110 min half-life of [^{18}F]-labeled precursors imposes serious limitations on the number of steps that can be accommodated in a radiochemical synthesis and generally prevents quality control assessment prior to dispensing for clinical use.

In light of the difficulties with [^{18}F]-labeling, DOTA-bioconjugates have become competitive alternatives in part because they are labeled by a one-step wash-in of aqueous [^{64}Cu]-cupric ion.[12,16] Although the preparation of a scalable and shelf-stable DOTA-bioconjugate presents clear advantages from a radiosynthetic perspective, [^{64}Cu]-copper affords suboptimal nuclear properties including lower specific activity, multiple decay processes, isotopic impurity,[25] and difficulty in production. In addition, [^{64}Cu]-DOTA and related chelates may transchelate [^{64}Cu]-cupric ion to endogenous proteins.[26] Ideally, one would envision a bioconjugate that could be labeled in a single, aqueous step using anionic [^{18}F]-fluoride instead of [^{64}Cu]-cupric ion.

To that end, a recent report exploited earlier work in Si−F bond formation[27−29] to demonstrate that a di-*tert*-butyl(*p*-benzaldehyde)-silyl-[^{19}F]-fluoride would undergo isotopic exchange with [^{18}F]-fluoride to provide a small organosilylfluoride synthon that was stable in vivo and did not solvolyze ^{18}F-fluoride to the bone (by comparison the triphenylsilylfluoride releases considerable amounts of ^{18}F-fluoride to the bone).[30] In the same report, an octreotide-di-*tert*-butyl(*p*-benzaldehyde)-silyl-[^{19}F]-fluoride conjugate (74 nmol/800 μL) underwent isotopic exchange with 6 mCi [^{18}F]-fluoride under no carrier added conditions to afford a radiochemical yield >75% and potentially very high specific activity (0.08 Ci/μmol), although the targeting ability of this conjugate remained undisclosed. Although no carrier added [^{18}F]-fluoride was used in the isotopic exchange, it is noteworthy that 74 nmol of carrier [^{19}F]-fluoride was already present in the precursor.

Contemporaneously with this insightful work on silylfluorides, we proposed the use of a pendant arylboronic ester functionality as a chemoselective captor of *aqueous* [^{18}F]-fluoride to afford an [^{18}F]-labeled aryltrifluoroborate anion (hereafter abbreviated as $ArBF_3^-$).[31] The idea that a fluorophilic boron atom on a bioconjugate could afford direct aqueous labeling represented a very different approach to the aforementioned C−F bond-forming strategies. In our initial report, we employed a high degree of added carrier [^{19}F]-fluoride to favor the synthesis of the $ArBF_3^-$ and went on to suggest, without evidence, that practical conditions could be found that would afford labeling with specific activities suitable for PET imaging.[31] Because low specific activities were initially used, no evidence for in vivo stability of the $ArBF_3^-$ was presented at the time.

Indeed if this approach is to be seriously entertained, minimally three conditions must be met. These are briefly

(19) For example, electrophilic "F^+" fluorinating reagents, e.g., Xe[^{18}F]$_2$, [^{18}F]$_2$, and N-fluorinated species are very reactive, and in consequence are neither particularly chemoselective nor very tolerant of aqueous conditions in which most biomolecules are stored. Additionally, these F^+-reagents are difficult to generate with high specific radioactivity. In contrast, anionic [^{18}F]-fluoride, while readily generated with very high specific radioactivity, remains virtually inert in water as a highly hydrated anion. Thus its incorporation into organic compounds generally requires scrupulously dry conditions often at elevated temperatures: conditions that are totally incompatible with most biomolecules.

(20) Garg, P. K.; Garg, S.; Zalutsky, M. R. *Bioconjugate Chem.* **1991**, *2*, 44.
(21) Grierson, J. R.; Yagle, K. J.; Eary, J. F.; Tait, J. F.; Gibson, D. F.; Lewellen, B.; Link, J. M.; Krohn, K. A. *Bioconjugate Chem.* **2004**, *15*, 373.
(22) Ross, T. L.; Ermert, J.; Hocke, C.; Coenen, H. H. *J. Am. Chem. Soc.* **2007**, *129*, 8018.
(23) Glaser, M.; Arstad, E. *Bioconjugate Chem.* **2007**, *18*, 989.
(24) Flavell, R. R.; Kothari, P.; Bar-Dagan, M.; Synan, M.; Vallabhajosula, S.; Friedman, J. M.; Muir, T. W.; Ceccarini, G. *J. Am. Chem. Soc.* **2008**, *130*, 9106–9112.
(25) Abbas, K.; Kozempel, J.; Bonardi, M.; Groppi, F.; Alfarano, A.; Holzwarth, U.; Simonelli, F.; Hofman, H.; Horstmann, W.; Menapace, E.; Leseticky, L.; Gibson, N. *Appl. Radiat. Isot.* **2006**, *64*, 1001.
(26) Boswell, C. A.; Sun, X.; Niu, W.; Weisman, G. R.; Wong, E. H.; Rheingold, A. L.; Anderson, C. J. *J. Med. Chem.* **2004**, *47*, 1465.
(27) Rosenthal, M. S.; Bosch, A. L.; Nickles, R. J.; Gatley, S. J. *Int. J. Appl. Radiat. Isot* **1985**, *36*, 318.
(28) Pilcher, A. S.; Ammon, H. L.; Deshong, P. *J. Am. Chem. Soc.* **1995**, *117*, 5166.
(29) Walsh, J. C.; Akhoon, N.; Satyamurthy, J. R.; Barrio, M. E.; Phelps, S. S.; Gambhir, T.; Toyokuni, T. *J. Labelled Compd. Radiopharm.* **1999**, *42*, S1.
(30) Schirrmacher, R.; Bradtmoller, G.; Schirrmacher, E.; Thews, O.; Tillmanns, J.; Siessmeier, T.; Buchholz, H. G.; Bartenstein, P.; Wangler, B.; Niemeyer, C. M.; Jurkschat, K. *Angew. Chem., Int. Ed.* **2006**, *45*, 6047.
(31) Ting, R.; Adam, M. J.; Ruth, T. J.; Perrin, D. M. *J. Am. Chem. Soc.* **2005**, *127*, 13094.

detailed: (1) Clean-up. As with the preparation of all radiopharmaceuticals, free [^{18}F]-fluoride must be removed from the [^{18}F]-labeled $ArBF_3^-$. (2) Specific activity. Because we deliberately add carrier [^{19}F]-fluoride to favor the synthesis of the $ArBF_3^-$, the specific activity would need to be sufficiently high to visualize in vivo clearance, and a convincing argument must be made that specific activities greater than 1 Ci/μmol can be realized. (3) In vivo stability, tissue distribution, and clearance. As with the aforementioned silylfluoride, the $ArBF_3^-$ must be kinetically stable in serum and moreover must neither solvolytically leach [^{18}F]-fluoride to the calcium-rich, fluorophilic bone nor accumulate therein (such accumulation would be difficult to distinguish from that of solvolyzed free [^{18}F]-fluoride).

Herein, we demonstrate that a biotinylated arylboronic ester can indeed be labeled with moderately high specific activity,[32,35] isolated from unincorporated free [$^{18/19}$F]-fluoride,[32,35] and PET imaged to indicate clearance predominantly to the bladder as well as to other organs, with neither loss of fluoride to the bone, nor accumulation therein. When bound to NeutrAvidin, the biotinyl-ArB[$^{18/19}$F]$_3$ manifests a visibly different pharmacokinetic clearance pattern and detectably different biodistribution, which further demonstrates the tunablity of this approach. The work herein validates B−F bond formation in the generation of potentially useful PET imaging agents that can be easily labeled with [^{18}F]-fluoride in one aqueous step.[31] The extent to which carrier [^{19}F]-fluoride is needed and to what extent its presence infringes on the specific activity needed for imaging is discussed in the conclusions (vide infra).

Thermodynamic and Kinetic Considerations. Because the hypothesis that arylboronic acids and esters can usefully capture aqueous [^{18}F]-fluoride for PET imaging is conceptually novel and unorthodox, we preface this work with a brief discussion of the thermodynamic and kinetic aspects of $ArBF_3^-$ preparation and their contemplated use in imaging, some of which have been made recently elsewhere.[33] As with all radiopharmaceuticals that are synthesized under very different conditions from the in vivo conditions in which they are ultimately investigated, an $ArBF_3^-$ is no different: it is prepared from $ArB(OR)_2$ at relatively low pH, for example 3−4, and at relatively high concentrations of aqueous fluoride, for example 100 mM, where at least 3 equiv of fluoride is used for each arylboronic ester/acid in keeping with the stoichiometry given in

$$ArB(OR)_2 + KF + 2HF \rightleftharpoons ArBF_3K + 2ROH \qquad (1)$$

The conversion of an arylboronic acid to the $ArBF_3^-$ is enhanced at low pH where solution acidity protonates the RO group (R = alkyl, H) to facilitate displacement by fluoride. Under these conditions, $ArBF_3^-$ formation is relatively fast, and in our hands, chemical yields with respect to boron have varied from 10−50% over the period of one hour at 25−37° (higher temperatures should enhance yields and rates). Because the specific activity of no carrier added [^{18}F]-fluoride is seldom greater than 100 Ci/μmol, and is usually considerably lower,[34] the resulting $ArBF_3^-$ will exist as a mixture of inseparable isotopologs comprising mainly unlabeled species and monolabeled species, hereafter denoted as ArB[^{18}F][^{19}F]$_2^-$ in the midst of less than 1% doubly labeled species and virtually no triply labeled species.

The $ArBF_3^-$ salt and any starting material is then resuspended in methanol and/or buffer at pH 7.5, whereupon no further conversion occurs on account of two effects (i) the elevated pH and (ii) the third-order equilibrium constant which upon significant dilution (total arylboron concentration ~1 to 5 mM upon resuspension, <1 μM upon injection) halts formation. As synthesis is arrested at this juncture, the $ArBF_3^-$ is henceforth capable of solvolytically reverting to the arylboronic acid and free fluoride. The thermodynamics of solvolytic reversion to free fluoride is governed by a third-order equilibrium constant:

$$K_{eq_{solv.pH7.5}} = \frac{[ArB(OH)_2][F^-]^3}{[ArBF_3^-]} \qquad (2)$$

When an $ArBF_3^-$ is diluted to ~5 mM in aqueous solution at pH 7.5, both the rate and extent of its dissociation to free fluoride can be measured by ^{19}F NMR spectroscopy.[33] By studying the solvolysis of a series of substituted $ArBF_3^-$s, we found that the thermodynamic equilibrium of solvolytic reversion to free fluoride and $ArBOH_2$ at pH > 7 is so strongly favored that no free $ArBF_3^-$ can be detected at equilibrium. Thus we concluded that $K_{eq\text{-}obs}$ is at least equal to unity if not considerably greater than unity, because even in the presence of 100 mM fluoride, the extent of $ArBF_3^-$ decomposition is not detectably diminished. Since K_{eq} is greater than unity and the rate equation describing $ArBF_3$'s formation is third order in fluoride, eq 2 also ensures that when the $ArBF_3^-$ is humorally diluted to <100 nM, the presence of any contaminating amount of unlabeled precursor $ArB(OR)_2$ that might conceivably be present postlabeling exerts an insignificant effect on the amount of free fluoride that will be released at equilibrium.

Despite the very favorable nature of $ArBF_3^-$ solvolysis at pH > 7, the rate of $ArBF_3^-$ solvolysis can range from very fast ($k_{obs} \approx 0.1$ min^{-1}) to very slow ($k_{obs} \approx 10^{-4}$ min^{-1}) depending on aromatic ring substitution as we have recently reported.[33] As such, we hypothesized that a suitably labeled $ArBF_3^-$ can still be used for PET imaging in cases where $ArBF_3^-$ persistence at dilute concentrations in water (or serum) can only be explained by kinetic stability. A correlation of ring substitution with hydrolytic stability led us to rationally design a fluorescent derivative of 1,3,5-trifluoro-2-carboxamido-phenyl-4-trifluoroborate that was labeled with [^{18}F]-fluoride in reasonable yields and investigated for its considerable kinetic stability in buffer pH ≈ 7; it manifested a slow but measurable rate of solvolytic [^{18}F]-fluoride exchange in the presence of excess 100 mM [^{19}F]-KF, pH 7.5 ($k_{obs} \approx 1.2 \times 10^{-4}$ min^{-1}).[35] On the basis of these data, we wished to examine the in vivo stability of a biotinylated version of the same $ArBF_3^-$, that is, biotinyl-ArB[^{18}F][^{19}F]$_2^-$ (**3**) and describe its radiofluoridation from its precursor arylboronic ester (**2**) as a captor for aqueous [^{18}F]-fluoride shown in Figure 1.

Results

The tetraphenylpinacolyl ester (**1**) was selected in part to afford clean chromatographic mobility and enhanced solubility during the EDC-mediated condensation with the biotinylated piperazine to afford the biotinylated boronate ester conjugate (**2**). To showcase the generality of this approach, we chose biotin as our test ligand because biotin has already been used as an imaging agent in numerous contexts, involving avidin and avidin fusion proteins.[8,9,18] At 432 mM fluoride, a relatively high

(32) Harwig, C. W.; Ting, R.; Adam, M. J.; Ruth, T. J.; Perrin, D. M. *Tetrahedron Lett.* **2008**, *49*, 3152.
(33) Ting, R.; Harwig, C. W.; Lo, J.; Li, Y.; Adam, M. J.; Ruth, T. J.; Perrin, D. M. *J. Org. Chem.* **2008**, *73*, 4662.
(34) Lasne, M. C.; Perrio, C.; Rouden, J.; Barre, L.; Roeda, D.; Dolle, F.; Crouzel, C. *Top. Curr. Chem.* **2002**, *222*, 201.
(35) Ting, R.; Lo, J.; Adam, M. J.; Ruth, T. J.; Perrin, D. M. *J. Fluorine Chem.* **2008**, *129*, 349.

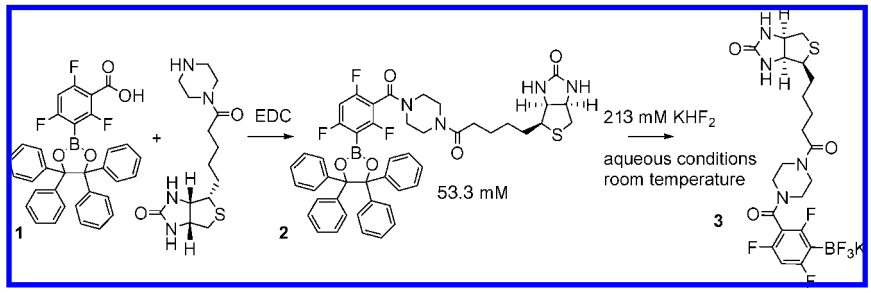

Figure 1. The free carboxylic acid of the tetraphenylpinacolyl arylboronate (**1**) is condensed with the biotinylated piperazine to give **2** which is readily converted to the biotinyl-ArB[^{18}F][^{19}F]$_2$ (**3**) at ~200 mM F$^-$.

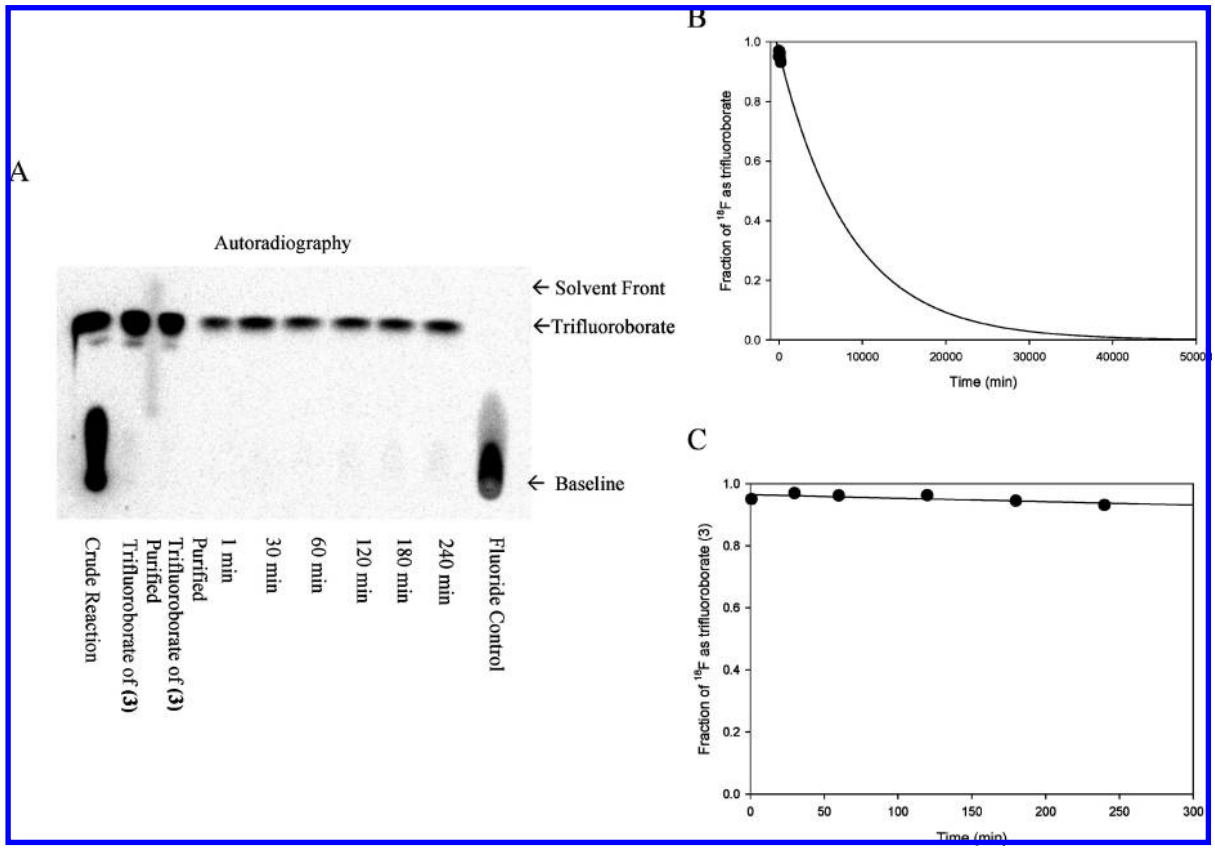

Figure 2. Time-dependent solvolytic exchange of the biotinyl-ArB[^{18}F][^{19}F]$_2^-$ (**3**) with excess [^{19}F]-fluoride. (A) Autoradiograph of the kinetic assay of [^{18}F]-fluoride loss from (**3**) as monitored by TLC in an isotopic exchange experiment, 5:95 NH_4OH/ethanol. The purified trifluoroborate (**3**) was spotted twice for reproducibility. (B) Plot of relative autoradiographic density corresponding to the biotinyl-ArB[^{18}F][^{19}F]$_2$ fraction vs time. Data were fit to the function $y = a(e^{-k_{obs}t})$, $k_{obs} = 0.00012 \pm 0.00006$, $a = 0.965 \pm 0.007$, $R^2 = 0.532$; $t_{1/2} = 5800 \pm 2000$ min. (C) Plot B rescaled relative to a period of 300 min.

concentration chosen to afford near-quantitative conversion at relatively short times, compound **2** could be converted to the corresponding biotinyl-ArB[^{18}F][^{19}F]$_2^-$ (**3**), which could be readily separated from free fluoride using a small silica column resolved with 5:95 NH_4OH/ethanol. Analysis of this sample by ^{19}F NMR spectroscopy confirmed three singlets and one quartet (integration 1:1:1:3) that corresponded to the three unique arylfluoride resonances and one aryltrifluoroborate resonance, respectively, and confirmed complete conversion of **2** to **3**. No free fluoride could be detected by ^{19}F NMR spectroscopy (data not shown) confirming that this purification removes unincorporated fluoride.[35]

To validate labeling biotin in a radiochemical context, we synthesized the biotinylated $ArBF_3^-$ in the presence of 1 mCi [^{18}F]-fluoride: 1.5 μL of a 200 mM solution of **2** (300 nmol) in DMF was added to 2.2 μL of a 363.6 mM KH[$^{18/19}$F]$_2$ (0.625 mCi/μmol, 1.6 μmol, 432 mM final [$^{18/19}$F]-fluoride) pH 4.5, and the reaction was allowed to proceed for 159 min at 37 °C at which point the reaction was quenched with 50 μL methanol and the reaction was applied to a dry silica column (0.5 cm diameter, 3 cm length) from which 22.7 μCi corresponding to the biotinylated-ArB[^{18}F][^{19}F]$_2^-$ (**3**) was eluted in the first 500 μL. This represents an isolated yield of 2.3% (decay uncorrected). Densitometry analysis of the crude reaction lane shown in Figure 2 indicated an observed (not isolated) radiochemical yield of just under 15%, calculated from autoradiography of free [^{18}F]-fluoride and the higher moving spot representing the [^{18}F]-labeled $ArBF_3^-$. As excess fluoride has been added, and because three fluoride atoms condense with one boron, the difference between a 15% observed yield and a 2.3% isolated yield is reconciled in detail with regards to the sample that was prepared for imaging in vivo.

Previously, we described in detail the development of an isotopic exchange assay to measure the time-dependent solvolytic exchange of the boron-bound fluoride atoms in the presence of large excess of [^{19}F]-fluoride.[12,33] Herein, we repeated the same assay with **3** to demonstrate consistency with our previous report on the aqueous stability of the same $ArBF_3^-$ linked to BODIPY.[35] Briefly, **2** was converted to labeled **3** and then purified away from free fluoride and stored in methanol. Aliquots were diluted to 0.5 mM in 100 mM [^{19}F]-KF and 192 mM phosphate buffer pH 7.5 and allowed to solvolyze for various periods of time. At the end of the assay, a volume of 1 μL from each exchange reaction was spotted on a TLC plate. The large excess of [^{19}F]-KF prevented any free arylboronic acid that had solvolytically liberated its fluoride from recapturing [^{18}F]-fluoride once the TLC plate had dried. The solvent system 5:95 NH_4OH/EtOH cleanly separated the $ArBF_3^-$ from free fluoride with an R_f of 0.9. This isotopic exchange experiment measures the kinetic stability of the labeled $ArBF_3^-$ under aqueous buffered conditions and reproduces the expected stability that had been previously observed for the same $ArBF_3^-$ when linked to BODIPY. The autoradiogram of the TLC, shown in Figure 2, demonstrates good radiochemical yield (lane 1), purity (lanes 2 and 3), and high aqueous stability (lanes 4−9, graphs B and C).

Because the [^{19}F]-KF at 100 mM is in large excess over all boron-containing species, this assay measures the kinetic stability of the labeled $ArBF_3^-$ irrespective of the presence of unlabeled $ArBF_3^-$ or precursor $ArB(OR)_2$. Because all samples were prepared using the same [^{18}F]-fluoride sample, the nuclear decay rate does not enter into the calculation of the observed rate constant for the exchange reaction because both $ArBF_3^-$ and free fluoride, which are cleanly separated on the TLC plate, decay at the same rate. The observed rate constant for solvolysis is necessarily pseudo-first-order because of the large excess of unlabeled fluoride.

Because *this* particular $ArBF_3^-$ is so sluggish to exchange its fluoride, very little exchange is observed during a period of 240 min and consequently there is considerable error associated with fitting the data either by (i) the method of initial rates (Figure 2, graph B) or (ii) to an exponential first-order decay that must necessarily approach 0% [^{18}F]-fluoride remaining in the $ArBF_3^-$ at infinity (Figure 2, graph C). Errors notwithstanding, the half-life for the solvolysis of this $ArBF_3^-$ is minimally 3800 min, suggesting that 10% of the fluoride will be solvolytically liberated in a period not shorter than 833 min, or approximately 7.5 half-lives of ^{18}F-decay.

To corroborate these values, the solvolysis of the more water soluble 1,3,5-trifluoro-2-carboxy-4-trifluoroborate was monitored by ^{19}F NMR spectroscopy and a k_{obs} was calculated to be $\sim 8 \times 10^{-4}$ min^{-1} (data not shown). On the basis of Hammett values, the 2-carboxylate at pH 7.5 is less electron-withdrawing than the corresponding carboxamidyl-biotin used here. Thus, a slightly higher k_{obs} for solvolysis is observed for the free carboxylate, which is consistent with the Hammett relationship that we have observed for k_{solv} and Hammett σ-values.[33]

To verify that avidin recognized the labeled biotin, 60 nmol of the labeled biotinyl-ArB[^{18}F][^{19}F]$_2^-$ (**3**) was mixed with tetrameric NeutrAvidin (Pierce) in a 4:1 molar ratio in a final mixture of 80% phosphate-buffered saline and 20% methanol for approximately 45 min at room temperature after which time 1 volume of nondenaturing sample buffer (50 mM Tris-HCl, pH 6.8, 10% w/v sucrose, 0.006% w/v bromphenol blue) was added and decreasing amounts of the sample were loaded onto a 12% SDS-PAGE gel. The gel was then transferred to Whatman filter paper and placed in close proximity to a phosphorimager screen for exposure at 4°. As a control, tetrameric NeutrAvidin was also incubated with fluorescent Biotin-Atto680 (Sigma), loaded onto a 12% SDS-PAGE gel, and visualized using a Licor Odyssey near-infrared fluorescence gel scanner. The results of this experiment are shown in Figure 3. These results confirm that (i) **3** can be complexed with avidin and electrophoretically resolved as the avidin-bound species (monomers, tetramers, and higher molecular weight aggregates) and (ii) that these bands in the gel correlate nicely with those revealed with the use of a fluorescent biotin.

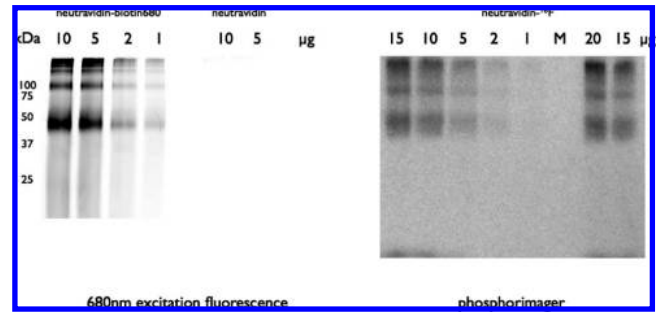

Figure 3. Polyacrylamide gel electrophoresis of NeutrAvidin. (A, left) Visualization by 680 nm excitation fluorescence of different amounts of NeutrAvidin bound to fluorescent biotin (left four lanes) and without biotin (right two lanes). (B, right) Visualization of different amounts of NeutrAvidin bound to biotinyl-ArB[^{18}F][^{19}F]$_2^-$ (**3**) by autoradiography. "M" denotes lane containing MW markers which are invisible in the autoradiography but on the original gel.

Encouraged by these results, we entertained an in vivo investigation of the labeled biotinyl-ArB[^{18}F][^{19}F]$_2^-$ (**3**) in the same manner as a previous study that addressed the stability of the di-*tert*-butyl(*p*-benzaldehyde)-silyl-[^{19}F]-fluoride. As previously noted, we were particularly concerned with whether signal would be observed in skeletal structures as such would reflect bone accumulation either because (**3**) solvolyzes to [^{18}F]-fluoride or simply accumulates therein. Although it is well-known that free [^{18}F]-fluoride readily and visibly accumulates in the bone and bladder, we injected 50 μCi of free ^{18}[F]-fluoride into the peritoneum of a mouse to generate a benchmark image to visualize large amounts of free fluoride localization in bone and the bladder. This image is shown below in Figure 4.

To prepare [^{18}F]-labeled-**3** with a specific activity needed for imaging we started with ~100 mCi of [$^{18/19}$F]-fluoride (800 nmols with a specific activity 0.125 Ci/μmol that gave a ratio of [^{18}F]/[^{19}F] $\approx 7.5 \times 10^{-5}$, at a final concentration of 213 mM total fluoride, at $t = 0$) and 200 nmol of **2** at a concentration of 53.3 mM which were allowed to react at room temperature for three hours. To calculate the correct specific activity for the isolated product and thus assess chemical and radiochemical yields, we noted that (i) the time delay of 180 min (1.64 half-lives) reduces the specific activity by a factor of 3.1; however, (ii) the stoichiometry by which three fluorides condense on each boron triples the specific activity of the resulting $ArBF_3^-$ compared to that of the fluoride used.[35] In *this* case, the effect of decay on specific activity following a 3 h reaction time is almost exactly negated by the stoichiometric enhancement factor of 3-to-1 such that final product had a specific activity of 0.121 Ci/μmol.

Starting with 100 mCi at $t = 0$, we isolated 2.3 mCi of biotinyl-ArB[^{18}F][^{19}F]$_2^-$ at $t = 180$ min which represents a *final* radiochemical yield of 2.3%, uncorrected for decay (decay

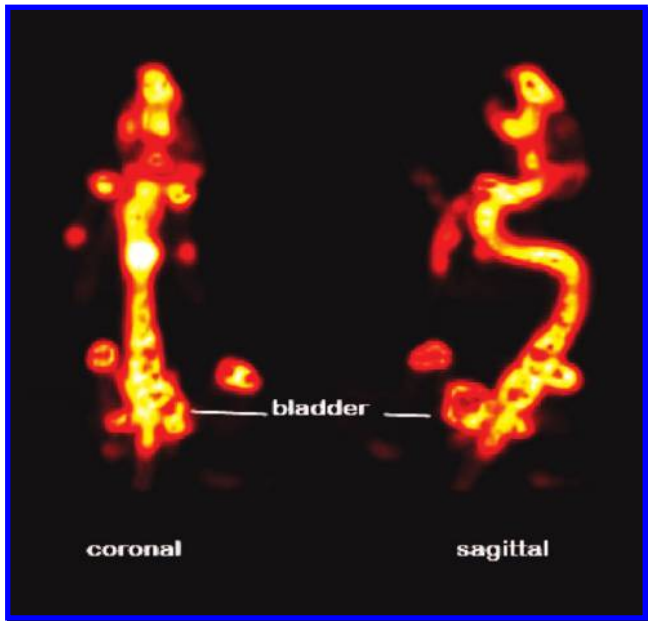

Figure 4. [^{18}F]-Free fluoride control figures that represent coronal (right) and sagittal (left) PET imaged mice imaged with an aqueous [^{18}F]-fluoride control buffered to pH 7.5 with sodium bicarbonate and injected as a 100 mM saline (NaCl) solution. Note the typical distribution of [^{18}F]-fluoride concentrates in the bladder and skeletal structures. Positron emission tomography images were reconstructed from images obtained 60 min postinjection. No transmission scan was acquired.

corrected yield of 7.1%) and an isolated yield of 18 nmol of biotinyl-ArB[^{18}F][^{19}F]$_2^-$. To further verify yield, an aliquot (<0.01%) of the crude reaction was subjected to analysis by TLC (see Supporting Information). The relative autoradiographic density from two spots corresponding to the free [^{18}F]-fluoride and biotinyl-ArB[^{18}F][^{19}F]$_2^-$ was measured using a phosphorimager. This autoradiographic analysis is independent of decay because both free [^{18}F]-fluoride and biotinyl-ArB[^{18}F][^{19}F]$_2^-$ decay at the same rate. From the autoradiography on the crude reaction, 10% of the autoradiographic density corresponds to the biotinyl-ArB[^{18}F][^{19}F]$_2^-$ which indicated a radiochemical incorporation of ~10% of the total fluoride. Thus 80 nmol of fluoride were incorporated from the starting 800 nmol, representing a radiochemical yield of 10%. Because each $ArBF_3^-$ contains three atoms of fluoride, the 80 nmol of incorporated fluoride is necessarily captured in 26.6 nmol of biotinyl-ArB[^{18}F][^{19}F]$_2^-$, which represents a nonisolated yield of 13%. When we isolated 2.3 mCi at $t = 180$ min at a specific activity of 0.121 Ci/μmol, this represents 18 nmol of labeled (**3**) and represents an isolated chemical yield of 9% with respect to boron. The 18 nmol of $ArBF_3^-$ carries 54 nmol fluoride which represents 6.75% of the total fluoride used and reflects a value not far from the isolated radiochemical yield of 7.1%, once corrected for decay based on the 2.3 mCi that were isolated. Within experimental error, the internal consistence of the chemical and radiochemical yields is reassuring.

From previous trial runs with low-level labeling reactions, we observed that the desired biotinyl-ArB[^{18}F][^{19}F]$_2^-$ (**3**) would elute from a short silica column run in 20:80 methanol/$CHCl_3$ after the first 10−15 fractions, and with a great deal of trailing (data not shown). Because we were working manually with a significant amount of radioactivity (20−100 mCi) and had no automatic fraction collector, we chose to minimize exposure by using 5:95 NH_4OH/ethanol, which afforded excellent removal of free [$^{18/19}$F]-fluoride and supplied the biotinyl-ArB[^{18}F][^{19}F]$_2^-$ in the first two 100 μL fractions. Nevertheless, the fractions that were collected were reresolved by analytical TLC using both 5:95 NH_4OH/ethanol and 20:80 methanol/$CHCl_3$ (see Supporting Information).

Because this study was undertaken largely to verify the stability of (**3**) in vivo, particularly with regards to assessing bone accumulation of hypothetically solvolyzed [^{18}F]-fluoride, or of (**3**) itself (vide infra), it was imperative to remove free [^{18}F]-fluoride for *this* preparation. Hence, we were not concerned with removing unlabeled biotin−boronate ester (**2**) because (i) it would be invisible to the PET scanner and more importantly (ii) because of the third-order equilibrium constant for $ArBF_3^-$ solvolysis (eq 2). Although the presence of precursor **2** at 1 μM has no effect on the overall release of fluoride from **3**, nevertheless, the presence of **2**, if not removed, reduces the specific activity. This concern is addressed in a discussion following the Conclusions section.

Following chromatographic isolation of 2.3 mCi of the biotinyl-ArB[^{18}F][^{19}F]$_2^-$ (**3**) in approximately 180 μL, we removed approximately 128 μCi (~10 μL) and added it either to 90 μL PBS and 100 μL NeutrAvidin (2 mg/mL) (12.5 nmol avidin monomer) to give one solution with avidin (solution A) or 190 μL PBS (phosphate buffered saline) to give one without avidin (solution B). A volume of ~150 μL solution A (~90 to 100 μCi) was injected into the tail vein of a 16 week old female Balb/c mouse. Thirteen minutes later, a volume of ~150 μL solution B (~90 to 100 μCi) was injected into the tail vein of a female litter-mate of the same species. This unfortunate delay occurred because standard laboratory protocol required tail vein injection prior to anesthesia. Because of this unforeseen time delay between the two mice, at the time that imaging commenced, the avidin−biotinyl-ArB[^{18}F][^{19}F]$_2^-$ had cleared for 13 min longer than the biotinyl-ArB[^{18}F][^{19}F]$_2^-$ itself.

Following injection, both mice were anesthetized and placed in the scanner for simultaneous imaging. A 90 min dynamic scan followed by a 10 min transmission scan was acquired and tomographic reconstruction generated the blue-hued images shown in Figure 5 (a video is enclosed in the Supporting Information). To account for this time delay and clearly present the images, we have reconstructed the still-life images in Figure 5 such that the each image represents the same time point—note that the earliest time point is 18 min.

In stark contrast to Figure 4, no accumulation in bone is ever observed. Instead, these data show that the biotinyl-ArB[^{18}F][^{19}F]$_2^-$ (**3**) clears rapidly and predominantly to the bladder with some accumulation in both the liver and salivary glands. Because of salivary gland excretion, signal is also observed in the bucal cavity (not brain). Some activity is observed in the stomach which is likely due to alimentary passage from the bucal cavity. Interestingly, the NeutrAvidin−biotinyl-ArB[^{18}F][^{19}F]$_2^-$ complex gave a different distribution image and a different kinetic profile with some apparent movement from the liver through what appears to be intestines or bile duct, particularly from 43 to 73 min. At the bottom of the right-hand image, one observes some symmetrical flares that are attributed to attenuation errors due to data reconstruction and not radioactive sample external to the subject.

In addition to these reconstructed images, we generated ex vivo standard uptake values (SUVs) and time activity curves (TACs) using the medical image data examiner program, Amide 0.8.19. As both mice were imaged simultaneously, the TAC data for the mouse that received only biotinyl-ArB[^{18}F][^{19}F]$_2^-$ reflects clearance starting at ~1 min whereas for the mouse that

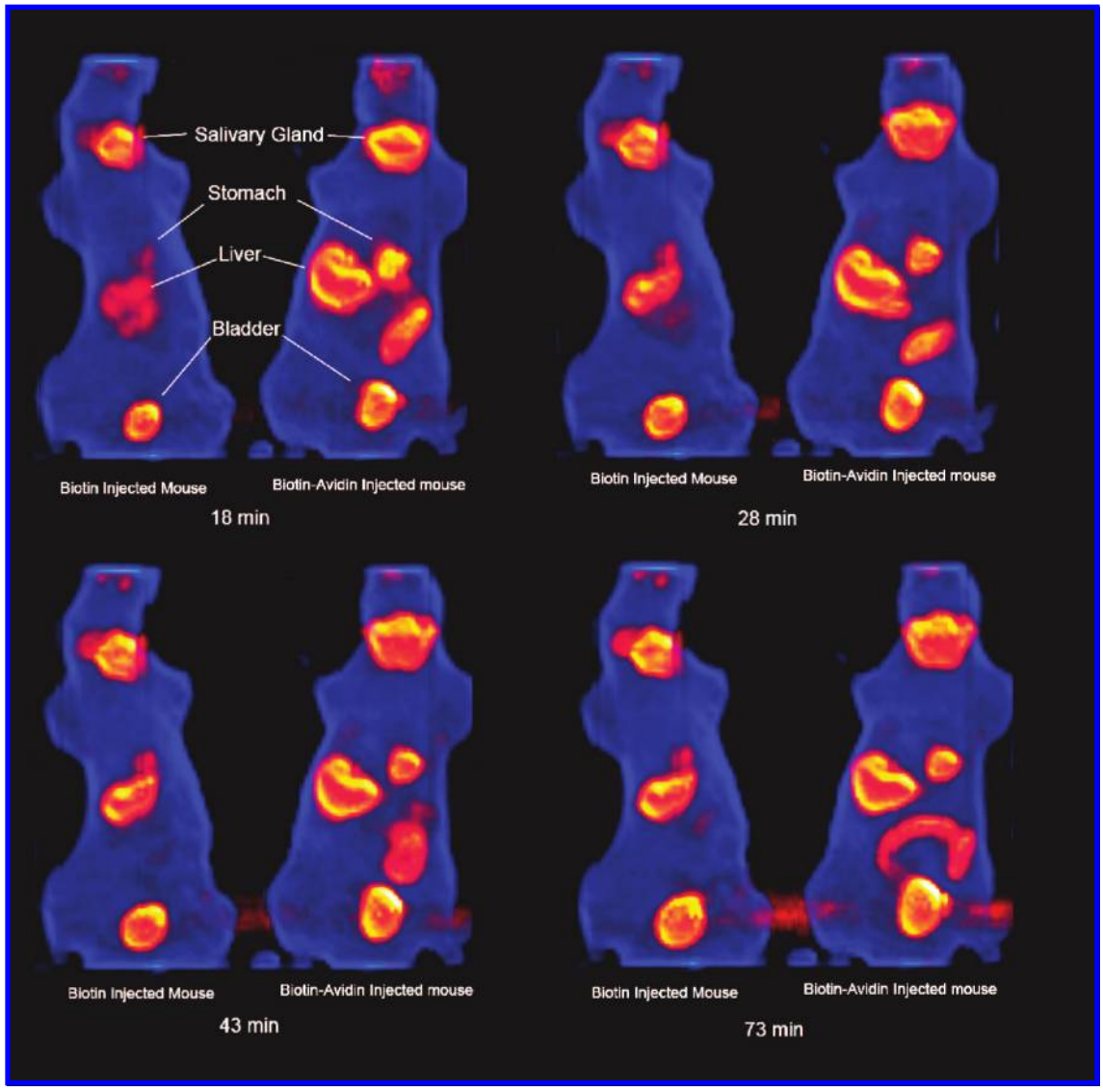

Figure 5. PET monitored distribution of the biotinyl-ArB[^{18}F][^{19}F]$_2^-$ (**3**) as free biotin and the biotin−avidin complex. PET scans showing the coronal and views of biotin and biotin-NeutrAvidin distribution at 0, 15, 30, and 90 min following the start of the PET experiment. Injection of the NeutrAvidin-bound composition occurred 13 min prior to the free biotinyl-ArB[^{18}F][^{19}F]$_2^-$.

received the NeutrAvidin−biotinyl-ArB[^{18}F][^{19}F]$_2^-$ complex, the clearance data reflects time points starting at ∼ 13 min post injection. For the purpose of reporting the TACs for both mice, the data were tabulated where $t = 0$ in terms of the time that the dynamic scan was started (again note a 13 min delay in bottom panel). Cubic volumes of 5 mm on each side (125 μL, ∼255 voxels each) were identified in various ROIs (regions of interest) within the 3D transmission scan to demonstrate uptake into the various organs in areas where signal is and is not observed (5 mm cubes are shown in the Supporting Information). Absolute values are given in the TACs and are not normalized to other tissues. As no skeletal bone structure could be identified under any conditions of contrast adjustment, two cubic ROIs, each at 255 voxels, were placed in the spinal region and in the pelvic region. Neither shows any time dependent increase in signal over background demonstrating that there is no uptake in bone. The TACs for both mice are shown in Figure 6.

Conclusions

Herein we validate our initial hypothesis that an arylboronic acid can be converted to an ArB[^{18}F][^{19}F]$_2^-$ in the presence of aqueous [$^{18/19}$F]-fluoride with sufficient specific activity that permits the first in vivo PET images of this composition. Following our initial report suggesting this methodology, it was imperative to demonstrate the in vivo stability and pharmacokinetic clearance of a labeled $ArBF_3^-$, particularly if its use is to be contemplated for imaging bone metastases which might be occluded if free fluoride were to solvolyze to the bone.

Although the work herein demonstrates in vivo $ArBF_3^-$ stability with regards to fluoride loss in but two animals ($n = 1$ for each, $n = 2$ if one assumes that the avidin has no effect on the $ArBF_3-$ stability), we have performed at least four other animals studies with an [^{18}F]-labeled 1,3,5-trifluoro-2-carboxamidyl-4-aryltrifluoroborate, either as the free acid or linked to marimastat, which is a broad-spectrum MMP inhibitor. In no case have we observed uptake in the bone (data not shown, manuscript in preparation). The data herein are thus fully consistent with the in vitro kinetic analyses presented herein and elsewhere along with a Hammett analysis that describes the kinetic stability of the $ArBF_3^-$ as a function of aryl substituent effects.[33]

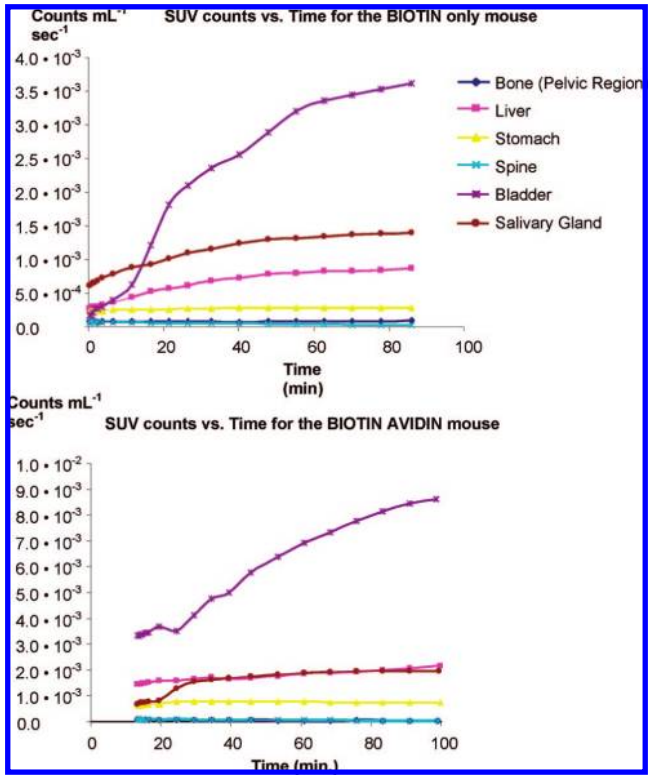

Figure 6. (Top) Time activity curve for various organs where uptake is observed in the biotin-only mouse. (Bottom) Time activity curve for various organs where uptake is observed in the avidin−biotin mouse. Signal is given in units of counts per mL per second.

Indeed, the main purpose of this work was to demonstrate the aqueous labeling of a biologically relevant $ArBF_3^-$ which had to be cleanly separated from free [^{18}F]-fluoride in order to assess its in vivo stability, particularly with regards to stability of the C−B bond and the B−F bonds: any release of fluoride from boron either directly via B−F solvolysis or indirectly via C−B fission to give the hydrolytically labile trifluoroborane (BF_3) would have resulted in free [^{18}F]-fluoride. Thus, it was essential to remove free [^{18}F]-fluoride from the $ArB[^{18}F][^{19}F]_2^-$. On the other hand, we were not immediately concerned with the presence of **2** as it was scintographically invisible. As already noted, the third-order nature of the K_{eq} for solvolysis ensures that the presence of **2** at submicromolar levels does not affect the solvolytic equilibrium of $ArBF_3^-$ and thus cannot explain why no signal is observed in the bone. Because of safety concerns, we opted to minimize exposure and thus chose a chromatographic solvent system that quickly removed the radiolabeled **3** from free [^{18}F]-fluoride but not from its precursor boronate **2**. Safety-related limitations notwithstanding, this work demonstrates for the first time that a suitably chosen [^{18}F]-labeled trifluoroborate is stable in vivo.

We chose to append biotin in this case as biotin is steadfastly becoming a convenient means of labeling other large molecules that have been fused to avidin. Having demonstrated the in vivo stability of the biotinyl-$ArB[^{18}F][^{19}F]_2^-$, we believe that compound **2** has the potential for immediate use in labeling other large molecules that are in some way fused to avidin.[8,9,18] The most salient aspect of these data is that the biotinyl-$ArB[^{18}F][^{19}F]_2^-$ appears to clear in vivo as a stable, noncoordinating anion with no apparent accumulation in the bone or solvolytic liberation of free [^{18}F]-fluoride that would have necessarily appeared therein. When **3** is precomplexed with avidin protein, the clearance is visibly altered, particularly in terms of drainage from the liver suggesting that we are indeed observing the clearance of the biotinylated-$ArBF_3^-$ with or without avidin.

Future Use of $ArBF_3$-Labeled Radiopharmaceuticals. Irrespective of a molecule's composition, upon infinite dilution, entropy renders *all* bond dissociation events both kinetically irreversible and thermodynamically favorable. In so far as humoral injection approximates infinite dilution, it is only the *kinetic* stability of the bond(s) joining the positron emitting isotope to the nonradioactive prosthetic group that governs the in vivo integrity of a radiopharmaceutical imaging agent. On this premise, one realizes that the bond dissociation energies of *all* bonds within the radiopharmaceutical may influence its in vivo stability as these may rupture spontaneously, be cleaved by circulating proteases, or altered by other metabolic enzymes. Such concerns necessarily add another level of complexity to the design of radiopharmaceuticals that are not solely limited to the bond dissociation energy of the positron emitting nucleide and whatever stable atom to which it is bound.

Although we cannot be absolutely certain of the metabolic fate of the biotinyl-$ArB[^{18}F][^{19}F]_2^-$, our main focus of this work has been the demonstration that the carbon−boron and boron−fluoride bonds are stable in vivo. Indeed if either C−B or B−F bond fragmentation had occurred, [^{18}F]-fluoride would have deposited in the bone, and such an observation could undermine future applications in developing boronic acids as useful PET precursors. Because the metabolic fate of *all* large radiopharmaceuticals can be further complicated by linker arm chemistries as well as the ligand to which it is attached, we have not fully investigated the metabolic fate of the 1,3,5-trifluoro-2-carboxamidyl-moiety of the $ArBF_3^-$ at this time. It is likely that issues of stability, if requiring attention, will only be meaningfully addressed in the context of other ligands that find use in imaging. In addition, in cases where this $ArBF_3^-$ may prove metabolically fragile, other EWG-modified $ArBF_3^-$s can also be investigated. On the basis of our Hammett analysis, we are confident that the tunability of the aryl ring for $ArBF_3^-$ stability will afford a plethora of $ArBF_3^-$s to potentially satisfy these secondary concerns for metabolic stability.

A noteworthy observation is that the $ArBF_3^-$ cleared very rapidly, an effect that has both advantages and disadvantages. On the one hand, the radiopharmaceuitical must circulate for a sufficient amount of time in order to reach its target, on the other hand, once the target has been reached, the unbound remainder should clear to afford a high signal-to-noise ratio. To what end this clearance rate can be modulated by the addition of other groups (cations, hydrophobic groups) will warrant further investigation. Nevertheless, this work demonstrates that other small molecules such as peptide hormones, folic acid, and oligonucleotides are readily conjugated to the precursor arylboronate ester (**1**) via standard amide couplings and will constitute a family of easily labeled bioconjugates, whose synthesis is currently underway in our laboratory. Such developments are currently being explored by us and will be reported in due time.

The Effect of Added Carrier on Specific Activity. Whereas this work demonstrated the in vivo stability of the C−B and B−F bonds in the context of this $ArBF_3^-$, we recognize that it is somewhat unusual to deliberately include carrier [^{19}F]-fluoride in the synthesis of a PET imaging agent. For those who may be skeptical of preparing PET-imaging agents in the presence of added carrier, here we critically address whether one could

obtain specific activities of >1 Ci/μmol that are generally required for imaging cellular targets. To begin to answer this question, it is worth noting that there appears to be a commonly held misconception that a no-carrier-added [^{18}F]-fluoride preparation will possess a specific activity anywhere close to the value of 1720 Ci/μmol for carrier-free [^{18}F]-fluoride. Any contemplation that radiopharmaceuticals can be labeled in carrier-free form with [^{18}F]-fluoride represents wishful thinking: the specific activity values for no-carrier-added preparations of [^{18}F]-fluoride are generally around 50 Ci/μmol due to environmental contamination by [^{19}F]-fluoride, which means that there is a significant amount of carrier [^{19}F]-fluoride present in a no-carrier-added preparation.[34] Even so, a specific activity of 50 Ci/μmol, which is relatively high for no-carrier-added preparations, is still 50-fold higher than the requisite specific activity of 1 Ci/μmol needed to image extracellular receptors. As such, a radiosynthesis starting with 1 Ci can actually accommodate the addition of 950 nmol of [^{19}F]-fluoride to bring the final amount of [$^{18/19}$F]-fluoride to 1 μmol.

At the outset of our synthesis (EOB) we used 100 mCi distributed in 800 nmol total [$^{18/19}$F]-fluoride (0.126 Ci/μmol, [^{18}F]/[^{19}F] ratio $\approx 7.5 \times 10^{-5}$) in 3.75 μL (213 mM fluoride). Correcting for both the time decay (1.64 half-lives) and the increase in specific activity due to the condensation of three fluoride atoms with one boron atom, we obtained a radiolabeled $ArBF_3^-$ with a specific activity of 0.12 Ci/μmol. In light of these results, it is not unreasonable to contemplate reactions in slightly lower volumes, for example 2 μL, where 800 mCi at 200 mM [$^{18/19}$F] (0.8 Ci/400 nmol) will afford specific activities of $\sim$2 Ci/μmol. Moreover because three fluoride atoms stoichiometrically condense to form one aryltrifluoroborate, this procedure necessarily triples the specific activity of the resulting $ArBF_3^-$ compared to the source fluoride. Consequently, the above conditions can facilely provide final specific activities on the order of 1$-$2 Ci/μmol aryltrifluoroborate, notwithstanding the decay that occurs following a 90 min reaction time. In addition, increasing the temperature of reaction and/or optimizing the solvent and pH conditions for labeling should reduce the labeling time and improve yields. Furthermore, the use of a microreactor that permits 100 nanoliter reaction volumes will afford at least 10$-$100 fold greater specific activities, as well as offering the possibility of working under no-carrier-added conditions while expecting reasonably high yields.[34]

It is also worth noting that, over the years, much emphasis has been placed on syntheses with no-carrier-added [^{18}F]-fluoride. It is imperative to recognize that the most important unit of specific activity is Ci/(μmol radiopharmaceutical), not Ci/(μmol fluoride), or even Ci/(μmol prosthetic group). In this regard, it is essential to consider the efficacy and need of separating labeled bioconjugate from unlabeled precursor. As is often the case, excess biomolecule is added in the last step to drive the bioconjugation reaction forward. If this precursor biomolecule cannot be separated from labeled bioconjugate its presence represents addition of carrier ligand, even if no carrier fluoride has been added.

Indeed, when unlabeled precursor copurifies with the radiolabeled product, the specific activity may decrease much further such that the addition of carrier fluoride will have little bearing on the specific activity Ci/(μmol radiopharmaceutical) needed for imaging. In the case of [^{18}F]-labeled insulin, the concern for the presence of excess unlabeled insulin was discussed and discounted as the authors suggested in vivo imaging studies would involve the addition of even more carrier insulin.[38] With regard to the work presented herein, the relatively modest chemical yield we observed with respect to boron *and* the currently ineffective separation from the biotinylated precursor (**2**) that we encountered resulted in a further lowering of the specific activity with respect to Ci/μmol biotin.

Although herein we chose not to remove the unlabeled biotinylated precursor, we anticipate that an automated chromatographic can be chosen to fully separate radiolabeled products from their unlabeled precursors using methanol/$CHCl_3$. Ultimately, interfacing a microreactor with a robotic chromatography apparatus will alleviate these aforementioned limitations on specific activity to safely allow us to fully realize the potential of using arylboronate esters as captors of aqueous [$^{18/19}$F]-fluoride in a generalized approach to the production of a broad scope of PET reagents with very high specific activities.

Materials and Methods

Chemicals were purchased from Sigma, Aldrich, or Acros Organic. Deuterated solvents were purchased from Cambridge Isotope Laboratories. Analytical and preparative thin layer chromatography experiments were run on Silica Gel 60 F_{254} Glass TLC plates from EMD Chemicals. All ^{1}H nuclear magnetic resonance (NMR) spectra were recorded on a Bruker Avance 300 or 400 MHz instrument. Chemical shifts are reported using the δ scale in ppm and all coupling constants (J) are reported in hertz (Hz). Unless specified, ^{1}H NMR spectra are referenced to the tetramethylsilane peak ($\delta = 0.00$) and ^{19}F NMR spectra are referenced to NEAT trifluoroacetic acid ($\delta = 0.00, -78.3$ ppm relative to $CFCl_3$). Because of the presence of [^{19}F]-fluoride contamination in the NMR spectrometer probe, baseline corrections for samples less than 20 mM in [^{19}F]-fluoride concentration had to be adjusted by multipoint linear baseline correction using MestReC 4.9.9.9. This correction did not affect the absolute chemical shifts or integration ratios of ^{19}F signals.

Piperazine Biotinamide. Biotin (0.34 g, 1.4 mmols) was dissolved in 8 mL of neat thionyl chloride. This reaction was allowed to proceed for 5 min before the reaction was placed under vacuum where excess thionyl chloride was removed. The resulting oil was resuspended in 10 mL of CH_2Cl_2 and dried down. This process was repeated three times to drive off excess thionyl chloride. A solution of piperazine (0.54 g, 6.3 mmols) dissolved in 30 mL of pyridine was added to the resulting oil. This solution was stirred overnight and concentrated, and the resulting solid was triturated with 40 mL of MeOH. The MeOH soluble material was collected by filtration, concentrated, and triturated with 40 mL of CH_2Cl_2. The CH_2Cl_2 soluble material was collected by filtration, concentrated, and chromatographed on a 1 cm silica column with 2:98 NH_4OH/ethanol as the running solvent. Elution was monitored by TLC where the product displays an R_f of 0.80 with a 33:67 NH_4OH/EtOH developing solution. The appropriate fractions were concentrated to give 42.9 mg of the piperazine biotinamide as a white solid in a 10% yield. ^{1}H NMR ($CDCl_3$, 300 MHz): 4.47$-$4.45 (m, 1H, C**H**^{23}), 4.30$-$4.26 (m, 1H, C**H**^{22}), 3.55 (m, 2H, C**H$_2$**^{14}), 3.42 (m, 2H, C**H$_2$**$^{14'}$), 3.14$-$3.12 (m, 1H, C**H**^{20}), 2.92$-$2.80 (m, 4H, C**H**^{13},), 2.43$-$2.30 (m, 4H), 1.71$-$1.61 (m, 4H), 1.45$-$1.40 (t, J = 7.4 Hz, 2H). HRMS (ESI) calculated for $C_{14}H_{24}N_4NaO_2S^+$ (M + Na)$^+$, 335.15121; found, 335.1516.

(36) Nevertheless, the fact is that biotinyl-ArB[$^{18/19}$F]$_3$ likely contained unreacted boronate ester (**2**); this would reduce the effective specific radioactivity with respect to all biotinylated species.

(37) A 500 mCi portion of no carrier added [^{18}F]-fluoride represents 5 nmol, which in 10 nL is a 500 mM solution of fluoride

(38) Guenther, K. J.; Yoganathan, S.; Garofalo, R.; Kawabata, T.; Strack, T.; Labiris, R.; Dolovich, M.; Chirakal, R.; Valliant, J. F. *J. Med. Chem.* **2006**, *49*, 1466.

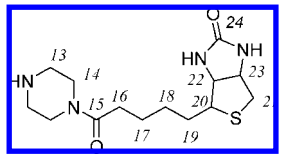

(2-(1,3,5-Trifluoro-4-(4,4,5,5-tetraphenyl-1,3,2-dioxaborolan-2-yl)benzoyl)piperazin-1-yl) Biotin (2). To a 4 mL vial containing 3.55 mL of DMF, were added in the following order: piperazine biotinamide (23.7 mg, 0.076 mmols), pyridine (33.2 μL, 0.41 mmols), HOBt monohydrate (13.5 mg, 0.10 mmols, **(1)** (50 mg, 0.09 mmols), (1,3,5-trifluoro-4-(4,4,5,5-tetraphenyl-1,3,2-dioxaborolan-2-yl)benzoic acid), prepared as described in Ting et al. *J Fluorine Chemistry*,[35] and EDC (19.4 mg, 0.10 mmols). This reaction was left for 16 h after which it was concentrated to oil and loaded onto a 0.5 cm silica column. Compound **2** was eluted with 10:90 MeOH/$CHCl_3$. Elution was monitored by TLC where **2** displays an R_f of 0.50 with a 30:70 MeOH/$CHCl_3$ developing solution. The appropriate fractions were concentrated to give 55.9 mg of **2** (73.3% yield) as a white solid. ^{1}H NMR (CD_2Cl_2, 400 MHz): 7.22 (*m*, 4H, C**H**^{9}), 7.21−7.20 (*m*, 4H, C**H**$^{9'}$), 7.14−7.11 (*m*, 12H, C**H**^{10,11}), 6.91 (*t*, *J*= 8.8 Hz, 1H, C**H**^{5}), 4.48 (*m*, 1H, C**H**^{23}), 4.31 (*m*, 1H, C**H**^{22}), 3.84−3.81 (*m*, 2H), 3.71−3.39 (*m*, 7H), 3.17 (*m*, 1H), 2.93−2.84 (*m*, 1H), 2.72−2.69 (*m*, 1H), 2.44−2.34 (*m*, 2H), 1.75- 1.68 (*m*, 4H), 1.29 (*m*, 2H). ^{19}F NMR (CD_2Cl_2, 300 MHz): −17.43 (1F), −22.61 (1F), −28.93 (1F). HRMS (ESI) calculated for $C_{47}H_{44}BF_3N_4NaO_5S^+$ $(M + Na)^+$, 867.29697; found, 867.2977.

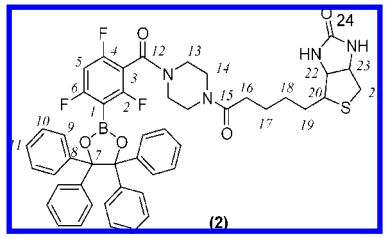

(2-(1,3,5-Trifluoro-4-(trifluoroboryl)benzoyl)piperazin-1-yl) Biotin (3). A ^{1}H NMR tube containing 475 μL of MeOH was charged with **2** (8.0 mg, 9.4 μmol) and 25 μL of a 4 M KHF_2 solution (200 μmol fluoride). The kinetic profile of trifluoroborate formation was monitored by ^{19}F NMR. The extent to which the reaction proceeded was gauged by the appearance of a trifluoroborate peak (TFB) at −59 ppm. Following completion of the reaction, the entire contents of the NMR tube were eluted through a Pasteur pipet packed with 600 mg of dry Silicycle 230−400 mesh silica. Compound **3** was eluted in the first 500 μL with 5% NH_4OH/EtOH as the eluant. This chromatography step facilitated the quantitative removal of free fluoride. ^{1}H NMR (MeOH-d4, 400 MHz): 6.66 (*t*, *J*= 9.2 Hz, 1H, C**H**^{5}), 4.48 (*m*, 1H, C**H**^{23}), 4.31 (*m*, 1H, C**H**^{22}), 3.85−3.80 (*m*, 2H), 3.73−3.35 (*m*, 7H), 3.25−3.20 (*m*, 1H), 2.93−2.90 (*m*, 1H), 2.72−2.69 (*m*, 1H), 2.49−2.41 (*m*, 2H), 1.75- 1.60 (*m*, 4H), 1.29 (*m*, 2H). ^{19}F NMR (5% NH_4OH/EtOH, 300 MHz): −20.70 (s, 1F, C**F**), −29.20 (s, 1F, C**F**), −41.23 (s, 1F, C**F**), −59.90 (br, 3F, B**F$_3$**). HRMS (ESI) calculated for $C_{21}H_{24}BF_6N_4O_3S^-$ $(M)^-$, 537.15718 *m*/*z*; found, 537.3.

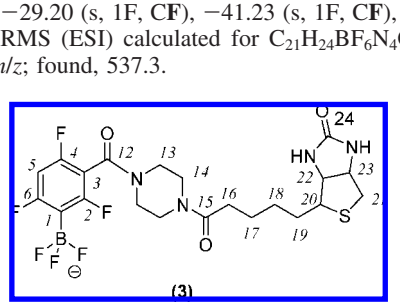

Radiochemical Procedures. ^{18}F Preparation. The desired activity of ^{18}F was prepared through the bombardment of 1 mL of $H_2{}^{18}O$ water with 12.5 MeV protons in a niobium target. To recover unconverted $H_2{}^{18}O$, the [^{18}F]-fluoride/$H_2{}^{18}O$ solution was passed through a short plug of anion-exchange resin (∼10 mg, CO_3^{2-} form). Resin bound fluoride was eluted with 200 to 300 μL of 1 mg/mL $NaClO_4$ and recovered in a glass vial. Depending on the desired activity, this sample could be diluted with deionized water, used as is, or excess water could be removed through heating under vacuum.

Low-Activity Radiochemical Synthesis of the Trifluoroborate of [$^{18/19}$F]-(3) for Gel Electrophoresis and Isotopic Exchange Experiments. A 1.95 mCi (t = 0 min) portion of [^{18}F]-fluoride was prepared from the proton bombardment of $H_2{}^{18}O$. This sample was dried and bought up with 2 μL of 2 M HCl to give a pH 3 solution. This solution was added to 1.5 μL of a 200 mM solution of **2** in DMF (300 nmols) before 0.2 μL of 4 M [^{19}F]-KHF_2 was added (1600 nmols F^-)(t = 16 min). The activity of this reaction mixture was 1 mCi (t = 30 min) (ca. 50% of activity was lost due to nonspecific binding). The fluoridation reaction was allowed to proceed at room temperature for 159 min, after which the reaction was quenched with 50 μL of MeOH and placed over a Pasteur pipet packed with 600 mg of dry 230−400 mesh silica. [$^{18/19}$F]-(**3**) was eluted with 500 μL of a 95:5 EtOH/NH_4OH solution and had an activity of 22.7 μCi (t =184 min). A radiochemical yield of 15% (∼75 nmols of [$^{18/19}$F]-(**3**)) was estimated from phosphorimaging analysis of the autoradiography of the crude reaction following TLC resolution. The purified fraction (∼500 μL) was centrifuged in an Eppendorf Microcentrifuge 5415C at 2000 rpm for 2 min and decanted from an SiO_2 pellet. This solution is heretofore called "sample-A". Six aliquots of 10 μL of sample-A were used in an [^{18}F]-isotope exchange experiment (vide infra). A 400 μL portion of sample-A was retained for polyacrylamide gel electrophoresis (vide infra).

[^{18}F] Isotope Exchange Experiments: Using the Low-Activity Radiochemical Synthesis of [$^{18/19}$F]-(3). To assay the dissociation rate of [^{18}F]-fluoride from the trifluoroborate **3**, the six aliquots of sample-A (each 10 μL, 1.5 nmol [$^{18/19}$F]-(**3**), 0.45 μCi (t = 184 min)) were diluted 30 fold into 300 μL of a 192 mM PO_4, pH 7.5, 100 mM [^{19}F]-NaF solution at different times. A volume of 0.5 μL of each dilution was spotted on a TLC plate which is run 2 in. in a 5:95 NH_4OH/ethanol developing solution. Each spot that was deposited on the plate had spent increasing amounts of time in the solution containing a vast excess of [^{19}F]-fluoride. Times in Figure 2 are reported as the time samples of [$^{18/19}$F]-(**3**) spent incubating in the phosphate−fluoride solution. Following autoradiography, a rate constant for the isotopic exchange of [^{18}F]-fluoride from [$^{18/19}$F]-(**3**) was calculated.[33,35]

Polyacrylamide Gel Electrophoresis Experiments: Using the Low-Activity Radiochemical Synthesis of [$^{18/19}$F]-(3). A 400 μL portion of sample-A, (60 nmol, 18.2 μCi (t = 184 min)) was mixed with tetrameric NeutrAvidin (Pierce) in a 4:1 molar ratio of biotin/avidin, such that the final solution was 80% phosphate-buffered saline and 20% ethanol at room temperature for 45 min (the ethanol came from the NH_4OH:ethanol solution used in the preceding chromatography). One volume of nondenaturing sample buffer was added and differing amounts of sample were loaded onto a 12% SDS-PAGE gel run at 100 V (12 W). Following electrophoresis, this gel was transferred to Whatman filter paper and exposed to a phosphorimager screen. As a control, tetrameric NeutrAvidin was also incubated with fluorescent Biotin-Atto680 (Sigma), loaded onto a 12% SDS-PAGE gel and visualized using a Licor Odyssey near-infrared fluorescence gel scanner.

High-Activity Radiochemical Synthesis of the Trifluoroborate of [$^{18/19}$F]-(3) for in Vivo Imaging. A 100 mCi (t = 0 min) portion of [^{18}F]-fluoride was prepared from the proton bombardment of $H_2{}^{18}O$. This sample was dried and bought up with a solution of 1.75 μL of 2 M HCl and 1 μL of 0.4 M KHF_2 to give a volume of 2.75 μL of a solution (pH of ∼3) containing 800 nmols of [$^{18/19}$F]-fluoride with a specific activity of 0.126 Ci/μmol (t = 0 min) at a concentration of 291 mM. This solution was added to 1

μL of a 200 mM solution of **2** in DMF ($t = 4$ min) to give a total volume of 3.75 μL reaction solution that was 53 mM in boron, 213 mM in [$^{18/19}$F]-fluoride, and 100 mCi ($t = 40$ min). The remainder of activity was apparently lost due to nonspecific binding and evaporation. This reaction was heated in a closed 600 μL eppendorf tube for 160 min at 41 °C, after which it was quenched with 30 μL of 95:5 EtOH/NH_4OH ($t = 160$ min) and eluted through a Pasteur pipet packed with 600 mg of dry 230−400 mesh silica. Five 100 μL fractions were collected using 95:5 EtOH/NH_4OH as the eluant. The first two fractions containing the majority of [$^{18/19}$F]-(**3**) were pooled and concentrated to 150 μL. In this pooled fraction, 2−2.3 mCi of [$^{18/19}$F]-(**3**) was obtained at $t = 160$ min, with a decay-corrected specific activity of 0.12 Ci/μmol, or 18 nmol of [$^{18/19}$F]-(**3**), corresponding to a chemical yield of 9% with respect to boron. This solution is heretofore referred to as "sample-B" and was taken to be 120 μM in labeled biotin. A volume of 10 μL of sample-B was added directly to 190 μL of phosphate buffered saline (pH 7.5) and transferred to the UBC hospital for tail vein injection. To image [^{18}F]-labeled NeutrAvidin, 10 μL of sample-B corresponding to 2−2.3 mCi of [$^{18/19}$F]-(**3**), ($t = 160$ min) and (1.2 nmol **3**) were added to 90 μL of phosphate buffered saline and 100 μL of 2 mg/mL NeutrAvidin (125 μM in monomeric avidin or 12.5 nmol monomeric avidin). A 150 μL (100 μCi, $t = 194$ min) portion of this sample was transferred to the UBC hospital for mouse tail vein injection.

In Vivo Biodistribution Studies. Two 10 week old female Balb/c mice were injected via the tail vein with ~127 and 100 μCi of either [$^{18/19}$F]-(**3**) or [$^{18/19}$F]-(**3**) preincubated with NeutrAvidin, respectively ($t = 194$ min). After injection the animals were anaesthetized with isofluorane (5% induction, 1.5% maintenance) and subjected to a 90 min dynamic scan followed by a 10 min transmission scan. There was a 13 min delay between each injection with the first mouse receiving [$^{18/19}$F]-(**3**) alone and the second mouse receiving the NeutrAvidin-complexed [$^{18/19}$F]-(**3**). PET data were compiled with Siemens Focus120 microPET software. PET images were generated with the open source program, Amide version 0.8.19.

Acknowledgment. R.T. was supported by Michael Smith and Gladys Estella Laird Fellowships, D.M.P. was awarded a Michael Smith Senior Career Scholar Award. This work was supported by operating and PoP grants of the CHIR. The authors thanks Ms. Salma Jivan for help in the preparation and elution of no-carrier added [^{18}F]-fluoride and Mr. Justin Lo for the synthesis of various biotinylated derivatives.

Supporting Information Available: Synthetic preparations, chromatography of labeled compounds, and critical NMR/HRMS traces; videos showing dynamic PET image, dynamic PET image with SUVs, static PET rotated image, static PET rotated image with SUVs, and ^{18}fluoride control. This material is available free of charge via the Internet at http://pubs.acs.org.

JA802734T